

Model-Based Investigation on the Mass Transfer and Adsorption Mechanisms of Mono-Pegylated Lysozyme in Ion-Exchange Chromatography

Josefine Morgenstern, Gang Wang, Pascal Baumann, and Jürgen Hubbuch*

Recent studies highlighted the potential of PEGylated proteins to improve stabilities and pharmacokinetics of protein drugs. Ion-exchange chromatography (IEX) is among the most frequently used purification methods for PEGylated proteins. However, the underlying physical mechanisms allowing for a separation of different PEGamers (proteins with a varying number of attached PEG molecules) are not yet fully understood. In this work, mechanistic chromatography modeling is applied to gain a deeper understanding of the mass transfer and adsorption/desorption mechanisms of mono-PEGylated proteins in IEX. Using a combination of the general rate model (GRM) and the steric mass action (SMA) isotherm, simulation results in good agreement with the experimental data are achieved. During linear gradient elution of proteins attached with PEG of different molecular weight, similar peak heights, and peak shapes at constant gradient length are observed. A superimposed effect of increased desorption rate and reduced diffusion rate as a function of the hydrodynamic radius of PEGylated proteins is identified to be the reason of this anomaly. That is why the concept of the diffusion-desorption-compensation effect is proposed. In addition to the altered elution orders, PEGylation results in a considerable decrease of maximum binding capacity. By using the SMA model in a kinetic formulation, the adsorption behavior of PEGylated proteins in the highly concentrated state is described mechanistically. An exponential increase in the steric hindrance effect with increasing PEG molecular weight is observed. This suggests the formation of multiple PEG layers in the interstitial space between bound proteins and an associated shielding of ligands on the adsorber surface to be the cause of the reduced maximum binding capacity. The presented *in silico* approach thus complements the hitherto proposed theories on the binding mechanisms of PEGylated proteins in IEX.

1. Introduction

It is estimated that in 2020 about 46% of the sales volume of the 100 highest selling pharmaceutical products will be achieved by biopharmaceutical products.^[1] Biopharmaceuticals contain active substances based on biological molecules, such as recombinant proteins. Compared to conventional small molecular pharmaceuticals, proteins have a complex three-dimensional structure allowing for a more efficient and specific intervention in cellular metabolic pathways. The efficacy of systemically administered protein drugs, however, may be hampered by a low bioavailability due to a poor solubility under physiological conditions, a short *in vivo* half-life due to a rapid elimination by the body and proteolysis. A promising approach to overcoming these drawbacks is the covalent attachment of polyethylene glycol (PEG) to protein drugs.^[2] As early as in 1977, the group of Abuchowski and Davis found an increased blood circulation half-life and a reduced immunogenicity of PEGylated proteins compared to the native form.^[3] Additional positive effects of PEGylation are an increased thermal stability as well as a higher solubility allowing for higher concentrated protein formulations.^[4] Two successfully approved PEGylated protein drugs are interferon α -2a (Pegasys,

Hoffman-LaRoche) for the treatment of hepatitis C and granulocyte-colony stimulating factor (Neulasta, Amgen) for the treatment of leukemia.

The emergence of conjugates with varying number (PEGamers) and site of attachment (positional isoforms) upon PEGylation reactions creates a need for a thorough purification in order to gain regulatory approval.^[5,6] Ion-exchange chromatography (IEX) is among the most frequently used purification methods for PEGylated proteins.^[5,7] Understanding the underlying physical mechanisms is an important prerequisite to optimize, control, predict, and scale-up the separation of PEGamers to pilot, and production level. In this context, mechanistic modeling provides an excellent opportunity to generate various information about mass transport and adsorption isotherm parameters *in silico*.

J. Morgenstern, G. Wang, Dr.-Ing P. Baumann,
Prof. Dr. J. Hubbuch
Institute of Engineering in Life Sciences, Section
IV: Biomolecular Separation Engineering
Karlsruhe Institute of Technology (KIT),
Engler-Bunte-Ring 3, 76131 Karlsruhe, Germany
E-mail: juergen.hubbuch@kit.edu

 The ORCID identification number(s) for the author(s) of this article can be found under <https://doi.org/10.1002/biot.201700255>.

© 2017 The Authors Biotechnology Journal Published by Wiley-VCH Verlag GmbH & Co. KGaA. This is an open access article under the terms of the Creative Commons Attribution-NonCommercial-NoDerivs License, which permits use and distribution in any medium, provided the original work is properly cited, the use is non-commercial and no modifications or adaptations are made.

DOI: 10.1002/biot.201700255

The physico-chemical properties and thus the behavior of a protein in chromatographic separation processes are significantly influenced by its PEGylation.^[5,6] Due to the high hydration of the hydrophilic PEG, PEGylated proteins have a distinctly higher hydrodynamic radius than unmodified proteins with the same molecular weight. A non-linear correlation introduced by Fee and Van Alstine allows a reliably mathematical prediction of the hydrodynamic radius $h_{R,PEGprot}$ based on the molecular weight of the protein and the attached PEG.^[5,8] In case of chromatographic separation, the PEG “cloud” around the protein results in an increased distance between protein binding site and adsorber surface.^[6] Seely and Richey^[9] observed that the elution order of different PEGamers was the same in both cation- and anion-exchange chromatography. They proposed the “charge-shielding effect” which links the weakened electrostatic interactions to the increased distance between protein binding site and adsorber surface. A deeper process understanding was achieved by Yamamoto et al.^[10] using mechanistic chromatography modeling. They applied the stoichiometric displacement model (SDM) to verify the “charge-shielding effect” quantitatively and associated it with the decreased elution volume of PEGamers. Moreover, it was shown that mono-PEGylated proteins are bound to the ion-exchange adsorber with binding sites similar to the unmodified protein. In following studies, this model was applied to PEGylated lysozyme and BSA.^[11,12] The aforementioned contributions demonstrated the successful application of mechanistic modeling to understand the adsorption behavior of PEGylated proteins in the linear region of the adsorption isotherm.

This work presents a full investigation of the behavior of mono-PEGylated proteins in IEX based on mechanistic chromatography modeling. In contrast to previous studies, information on the adsorption and desorption behavior in the non-linear region of the isotherm, i.e., the overloaded state, is included by using the steric mass action (SMA) model^[13] in kinetic formulation. Compared to the equilibrium isotherm used hitherto, the kinetic formulation is suitable for the description of protein behavior in higher concentrated state on adsorber surface. To further account for mass transfer effects within the chromatography column the general rate model (GRM)^[14] is employed. To best of our knowledge, mechanistic modeling of polymer grafted proteins in IEX using a combination of GRM and SMA isotherm has not been studied. By connecting these two approaches, this study delivers supplements by the quantitative investigation on the film diffusion, pore diffusion, charge, and shielding parameters, as well as the adsorption and desorption rate coefficients.

The model protein lysozyme from chicken egg was chosen as PEGylation target and conjugated to activated PEG of three different molecular weights (2, 5, and 10 kDa). The preparative isolation of the mono-PEGylated species was carried out using a single cation-exchange (CEX) chromatography step. For each purified protein species, four linear gradient elution (LGE) experiments with different gradient slopes were conducted to confirm the constancy of the characteristic charge. Breakthrough experiments were carried out to gain insight into the binding behavior of PEGylated proteins in the highly non-linear region and to investigate whether the perceivable behavior of PEGylated proteins originates from adsorption/desorption or mass transfer.

Confidence intervals at 95% level were calculated for parameter estimates.

2. Experimental Section

2.1. Adsorber, Proteins, and Chemicals

All stock solutions and buffers were prepared with ultra-pure water (PURELAB Ultra water purification system, ELGA Labwater, Germany), filtrated using a cellulose-acetate filter with a membrane cut-off of 0.22 μm (Satorius, Germany) and degassed by sonication. The used buffer substances were sodium acetate trihydrate (Sigma–Aldrich, USA) for pH 5 and sodium phosphate monobasic dihydrate (Sigma–Aldrich) as well as di-sodium hydrogen phosphate dihydrate (Merck, Germany) for pH 7.0 and 7.2, respectively. Hydrochloric acid and sodium hydroxide (NaOH) for pH adjustment were obtained from Merck (Germany). Lysozyme from chicken egg-white (no. HR7-110) was purchased from Hampton Research (USA). Methoxy-PEG-propionaldehyde (mPEG-aldehyde) with an average molecular weight (MW) of 2 kDa (Sunbright[®]ME-020 AL), 5 kDa (Sunbright[®]ME-050 AL) and 10 kDa (Sunbright[®]ME-100 AL) was obtained from NOF Corporation (Japan). Sodium cyanoborohydride (NaCNBH_3) and L-lysine were purchased from Sigma–Aldrich. For preparative isolation of PEGamers as well as for modeling purposes, the strong cation-exchange (CEX) chromatography adsorber medium TOYOPEARL[®] GigaCap S-650M (Tosoh Bioscience, Germany) was used. It is a high capacity polymer grated cation exchange resin based on hydroxylated methacrylic polymer with a 100 nm pore size and a 75 μm particle size. For preparative isolation of PEGamer species, 5 mL pre-packed MiniChrom columns (dimension: 100 mm \times 8 mm) and for modeling purposes, a pre-packed 0.965 mL Toyoscreen[®] column (dimension: 30 mm \times 6.4 mm) were used. Between the runs, the resin media were stored in 20% ethanol. The storage solution was removed by prolonged equilibration with ultra-pure water and flushed with binding and elution buffer before experimentation. Sodium chloride (NaCl) used for protein elution was purchased from Merck. A total of 0.5 M NaOH (Merck) was used for cleaning-in-place.

2.2. Instrumentation and Software

pH adjustment of all buffers was performed using a five-point calibrated pH-meter HI-3220 (Hanna Instruments, USA) equipped with a SenTix[®]62 pH electrode (Xylem, Inc., USA). Protein concentration measurements were conducted using a NanoDrop2000c UV–vis spectrophotometer (Thermo Fisher Scientific, USA). Purity of isolated mono-PEGylated lysozyme was determined by high-throughput capillary gel electrophoresis (HT-CGE) using the Caliper LabChip[®]GX II device (PerkinElmer, USA). For data processing and purity determination, the LabChip[®]GX 3.1 software (PerkinElmer) was used.

Preparative isolation of mono-PEGylated lysozyme species was performed on an ÄKTA[™] purifier system equipped with a Fraction Collector Frac-950 (GE Healthcare, Sweden). All experiments for chromatography model calibration were

carried out using an Ettan liquid chromatography (LC) system with the UV monitor UV-900 (3 mm optical path length), pump unit P-905, dynamic single chamber mixer M-925 (90 μ L mixer volume), and conductivity cell pH/C-900 (all GE Healthcare, Little Chalfont, Buckinghamshire, UK). The UNICORN 5.31 software (GE Healthcare, UK) was used to control both chromatographic systems and to record the signals. The protein chromatography simulation software ChromX (GoSilico, Germany) was used for the numerical simulations of the system of partial differential equations, estimation of model parameters, as well as for statistical analysis.^[15] Other data evaluations were conducted in Matlab[®] R2016a (MathWorks, USA).

2.3. PEGylation Reaction

As reaction buffer 25 mM sodium phosphate (pH 7.2) containing 20 mM sodium cyanoborohydride (NaCNBH₃) as reducing agent was used. PEGylation experiments were performed batch-wise in 50 mL Falcon Tubes (BD Biosciences, USA). Lysozyme (5 mg mL⁻¹) and mPEG-aldehyde were dissolved in the reaction buffer with a molar polymer to protein ratio of 6.67:1.^[16,17] The tube was continuously shaken in an overhead shaker LabincocoLD79 (Labincoco BV, the Netherlands) for 3.5 h at 25 °C. The PEGylation reaction was stopped by adding 200 mM of L-lysine according to Ref.^[18].

2.4. Preparative Purification of Mono-PEGylated Lysozyme

For preparative isolation of mono-PEGylated lysozyme, the stopped PEGylation batch was diluted to a ratio of 1:12 in 10 mM sodium acetate buffer (pH 5).^[16] For column loading, the system was equilibrated in 10 mM sodium acetate buffer (pH 5). Sample application was performed using a 50 mL super loop (GE Healthcare, Sweden). Elution was initiated by applying an NaCl step gradient with 10 mM sodium acetate buffer (pH 5) containing 1.0 M sodium chloride. The NaCl molarities used for the step elution of the different PEGamers are displayed in **Table 1** as a function of the molecular weight of the attached PEG molecules. The flow rate for binding and elution was set to 1 mL min⁻¹. Fractions of 2 mL were collected into a 96-well deep well plate (VWR, USA). To obtain sufficient sample volume for the linear gradient and the breakthrough experiments, fractions containing mono-PEGylated lysozyme of multiple chromatography runs were pooled.

Table 1. NaCl steps in mM used for the elution of different PEGamer species from Toyopearl GigaCap S-650M at pH 5 as a function of the PEG molecular weight.

	Native lysozyme	Mono-PEGylated lysozyme	Di-PEGylated lysozyme
2 kDa	1000	460	290
5 kDa	1000	350	160
10 kDa	1000	250	75

To ensure similar binding conditions for all PEG molecular weights during the calibration runs, the mono-PEGylated samples were concentrated to approximately $3.76 \cdot 10^{-4}$ M. This was accomplished by evaporation using a vacuum concentration unit RVC 2-33CDplus (Martin Christ Gefriertrocknungsanlagen GmbH, Germany) operated at 24 mbar. After concentrating, the protein samples were transferred to 25 mM sodium phosphate buffer (pH 7) using Slide-A-Lyzer[™] Dialysis Cassettes (Thermo Fisher Scientific) with a molecular weight cut-off of 2 kDa. All chromatography experiments were carried out at 25 °C.

2.5. Offline Identification and Quantification of PEGamer Species

Purity of isolated mono-PEGylated lysozyme was determined by high-throughput capillary gel electrophoresis (HT-CGE) as described in Ref.^[16]. The experiments were performed with an HT Protein Express LabChip[®] and an HT Protein Express Reagent Kit (Perkin Elmer, Hopkinton, MA, USA). The LabChip[®] installation, sample preparation, and analysis were performed according to the manufacturer's standard protocol.^[19] Sample preparation was performed in skirted 96-well polypropylene twin.tec[®] PCR plates from Eppendorf (Hamburg, Germany). Molecular weight determination was performed according to protein standards from the HT Protein Express Reagent Kit.

For protein quantification, absorption measurements at 280 nm were performed. Since the bound PEG molecules do not absorb at 280 nm, the extinction coefficient of $\epsilon_{280 \text{ nm, lysozyme}}^{1\%} = 22.00$ was used for native as well as for mono-PEGylated lysozyme.^[16,20] Appropriate blanks were subtracted. Molar concentrations were calculated using a lysozyme molecular mass of 14.6 kDa.^[21] The final concentrations of native lysozyme and mono-PEGylated species attached with 2, 5, and 10 kDa PEG used for the linear gradient and breakthrough experiments were $3.87 \cdot 10^{-4} \pm 7.19 \cdot 10^{-7}$ M, $3.63 \cdot 10^{-4} \pm 1.41 \cdot 10^{-7}$ M, $3.60 \cdot 10^{-4} \pm 1.61 \cdot 10^{-7}$ M, and $3.81 \cdot 10^{-4} \pm 1.57 \cdot 10^{-5}$ M, respectively. The slight deviations in PEGamer concentrations are due to concentrating and buffer exchange. For subsequent modeling the exact concentrations were employed.

2.6. Chromatography System Characterization

Tracer pulse injections at constant flow rate of 0.33 mL min⁻¹ were carried out to characterize the ÄKTA[™] system and chromatography column. For determination of the interstitial volume of the column, 25 μ L of 10 g L⁻¹ non-interacting, non-pore-penetrating tracer blue dextran 2000 kDa (Sigma-Aldrich, St. Louis, MO, USA) in ultra-pure water was used. Twenty-five microliters of 1% (v/v) pore-penetrating, non-interacting tracer acetone (Merck, Darmstadt, Germany) in ultra-pure water was used to determine system and total voidage of the column. The UV signals at 260 nm were recorded for that purpose. All measurements were corrected with respect to system dead volumes. The ionic capacity Λ of GigaCap S-650M was determined via acid-base titration following Huuk and co-workers.^[22]

2.7. Linear Gradient Experiments for Model Calibration

Protein solutions with lysozyme and its PEGylated species were prepared in binding buffer (25 mM sodium phosphate buffer, pH 7.0). Before injection, the protein solutions were filtrated with a membrane cut-off of 0.22 μm .

Linear gradient elution (LGE) experiments were used for determining model parameters for native lysozyme, lysozyme attached with PEG 2 kDa, PEG 5 kDa, and PEG 10 kDa. Protein solutions were injected via a 100 μL loop. After a post-loading wash step of 1 CV binding buffer, elution was carried out by increasing the salt gradient from 0 M to 1.0 M NaCl. From low-salt and high-salt buffer, linear gradients with a gradient length of 15 CV, 20 CV, and 25 CV were mixed within the LC system. After that, the column was stripped over 3 CV at an NaCl concentration of 1.0 M and re-equilibrated for 5 CV binding buffer. To ensure a constant residence time, all experiments were carried out at a flow rate of 0.33 mL min^{-1} .

2.8. Breakthrough Experiments for Model Calibration

Breakthrough experiments were used for modeling of the SMA isotherm model in the non-linear region. Protein solutions with native lysozyme, lysozyme attached with PEG 2 kDa, PEG 5 kDa, and PEG 10 kDa were prepared in binding buffer and injected via a 50 mL superloop (GE Healthcare, UK). The loading was carried out under strong binding condition at 0 M NaCl until 100% breakthrough was observed. To ensure a constant residence time, all experiments were carried out at a flow rate of 0.33 mL min^{-1} .

2.9. General Rate Model

In the presented study, the general rate model (GRM) was employed to cover convection and diffusion within a one-dimensional chromatography column of length L . Here, the concentrations of all components i in the bulk phase c , in the pore phase c_p , and adsorbed to the stationary phase q depend on time t and axial position x . Eq. 1 describes the mass transfer between the bulk phase and the pore phase depending on the flow velocity u , axial dispersion D_{ax} , bed porosity ϵ_b , film diffusion coefficient $k_{fil,m,i}$, particle radius r_p , and the concentrations c and c_p . The chosen Danckwerts boundary conditions are shown in Eqs. 2 and 3. In Eq. 4, the mass transfer between the pore phase and the stationary phase is described to be dependent on the radial position in the pore r , pore diffusion coefficient D_{pore} , particle porosity ϵ_p , film diffusion coefficient $k_{fil,m}$, and concentrations in the bulk phase c , pore phase c_p , and stationary phase q .

$$\frac{\partial c_i(x,t)}{\partial t} = -u(t) \frac{\partial c_i(x,t)}{\partial x} + D_{ax} \frac{\partial^2 c(x,t)}{\partial x^2} - \frac{1 - \epsilon_b}{\epsilon_b} k_{fil,m,i} \frac{3}{r_p} (c_i(x,t) - c_{p,i}(x,t)) \quad (1)$$

$$\frac{\partial c_i(0,t)}{\partial x} = \frac{u(t)}{D_{ax}} (c_i(0,t) - c_{imi}(t)) \quad (2)$$

$$\frac{\partial c_i(L,t)}{\partial x} = 0 \quad (3)$$

$$\frac{\partial c_{p,i}(x,t)}{\partial t} = \begin{cases} \frac{1}{r^2} \frac{\partial}{\partial r} \left(r^2 D_{p,i} \frac{\partial c_{p,i}(x,t)}{\partial r} \right) - \frac{1 - \epsilon_p}{\epsilon_p} \frac{\partial q_i(x,t)}{\partial t} & \text{for } r \in (0, r_p), \\ \frac{k_{fil,m,i}}{\epsilon_p D_{p,i}} (c_i(x,t) - c_{p,i}(x,t)) & \text{for } r = r_p, \\ 0 & \text{for } r = 0. \end{cases} \quad (4)$$

2.10. Adsorption Isotherm Model

Based on the stoichiometric displacement model (SDM),^[23] Brooks and Cramer derived the steric mass action (SMA) isotherm model by introducing the shielding factor σ , which accounts for the sterically hindered binding sites on the adsorber surface due to protein binding.^[13] In Eq. 5, the kinetic formulation according to Nilsson and co-workers is shown.^[24] It describes the protein concentration in the stationary phase q as a function of q itself, in the pore phase c_p , and salt concentration $c_{p,salt}$ in the pore phase.

$$k_{kin,i} \frac{\partial q_i(x,t)}{\partial t} = k_{eq,i} \left(\Lambda - \sum_{j=1}^k (v_j + \sigma_i) q_j(x,t) \right)^{v_i} c_{p,i}(x,t) - c_{p,salt}(x,t)^{v_i} q_i(x,t) \quad \forall i \neq \text{salt} \quad (5)$$

Equation 6 describes the salt concentration in the stationary phase as a function of proteins bound to the adsorber surface.

$$q_{salt}(x,t) = \Lambda - \sum_{j=1}^k v_j q_j(x,t) \quad (6)$$

Instead of the adsorption rate coefficient k_{ads} and the desorption rate coefficient k_{des} , the equilibrium coefficient $k_{eq} = k_{ads} k_{des}$ and the kinetic coefficient $k_{kin} = 1/k_{des}$ were used. In this way, parameter estimation was simplified, since k_{eq} and k_{kin} correlate mainly with the retention time and peak height, respectively.^[15] v is the characteristic charge, also known as the number of binding sites directly involved in binding. Λ is the column-specific ionic binding capacity equal to the number of potential binding sites. Here, the SMA isotherm has been chosen to cover the overloading state in investigated breakthrough experiments. For the description of low protein loading as usually applied in the step gradient experiments for preparative separation, the SDM isotherm would be sufficient. The kinetic formulation has been chosen out of several reasons. According to Carta and Jungbauer, protein adsorption is often slower than small molecules because of limitations in the binding kinetics. In addition, a true adsorption equilibrium may

not be established since the protein may undergo molecular changes due to unfolding, aggregation, or degradation before reaching equilibrium with the surface.^[25] Furthermore, Toyopearl GigaCap S-650M is a hydroxylated methacrylic polymer based and polymer grafted adsorber providing high ligand density. As result, fast adsorption rates may be favored initially, but with increasing protein binding, steric crowding and electrostatic repulsion may limit the access to binding sites.^[26,27]

2.11. Numerical Methods

The chromatograms resulting from LGE and breakthrough experiments were used to estimate the parameters with the inverse method.^[28] The adaptive simulated annealing (ASA)^[29] yielding the first guess was followed by the Levenberg–Marquardt (LM) algorithm^[30] for the fine adjustment of the parameter estimates. Subsequently, the confidence intervals at 95% level were calculated to verify estimation reliability. Discretization in space on a grid with equidistant nodes and θ -scheme discretization in time were carried out by employing the finite element method and the fractional step,^[31] respectively. Picard iteration was employed to approximate the solution of the non-linear equation system.^[32]

3. Results

3.1. PEGylation and Purification

In case of lysozyme, six lysine residues and the N-terminal amino group are available as binding sites for the PEG aldehyde reaction.^[33] The large number of binding sites allows for the formation of different PEGamers. Preparative isolation of the mono-PEGylated species was performed by a single cation-exchange step. In **Figure 1** the resulting chromatograms are shown for 1:12 diluted PEGylation batches with 2 kDa (a), 5 kDa (b), and 10 kDa (c) PEG. After peak fractionation, HT-CGE analysis was performed according to Ref. ^[16] to verify purity and PEGylation degree. As observed and discussed by Refs. ^[7,9,34], a decrease in elution volume with increasing PEGylation degree was observed for all PEG molecular weights. The red areas in

Figure 1a–c indicate the respective pooling limits for the mono-PEGylated species based on purity requirements greater than 97%. Purity was determined by HT-CGE analysis according to the analytical protocol established by Ref. ^[16]. The resulting fluorescence signals of HT-CGE for the native lysozyme and the purified mono-PEGylated species with a concentration of $6.99 \cdot 10^{-5}$ M showed a distinct peak broadening of PEGylated proteins compared to the native species (**Figure S1**, Supporting Information). In **Figure 2** the resulting fluorescence signals of HT-CGE are displayed for the native lysozyme and the purified mono-PEGylated species with a concentration of $6.99 \cdot 10^{-5}$ M. In accordance with,^[16] the results of the HT-CGE analysis showed a distinct peak broadening of PEGylated proteins compared to the native species. By using the calibration established by Ref. ^[16], this peak broadening was taken into account in the calculation of purities.

3.2. System Characteristics

Tracer experiments were carried out to determine the system parameters bed voidage, particle voidage, and axial dispersion. The ionic capacity was determined by applying acid-base titration. The results are shown in **Table 2**. The axial dispersion was found to be similar to the literature data.^[35]

3.3. Linear Gradient Elution and Breakthrough Experiments

Linear gradient experiments were carried out to generate information about proteins in the linear region of the adsorption isotherm. The retention time of every protein species over three different salt gradient lengths yielded information about the isotherm parameters characteristic charge ν and equilibrium coefficient k_{eq} . The height, width, and shape of the elution peaks provided partial information about the mass transfer parameters film diffusion coefficient k_{film} and pore diffusion coefficient D_{pore} . Thus, by employing ASA and LM, ν and k_{eq} were estimated with high reliability, for k_{film} and D_{pore} an initial guess was delivered. As can be seen by comparing the dashed lines in **Figure 2a, d, g, and j**, lysozyme in its native form was the strongest binding species for all investigated gradient lengths.

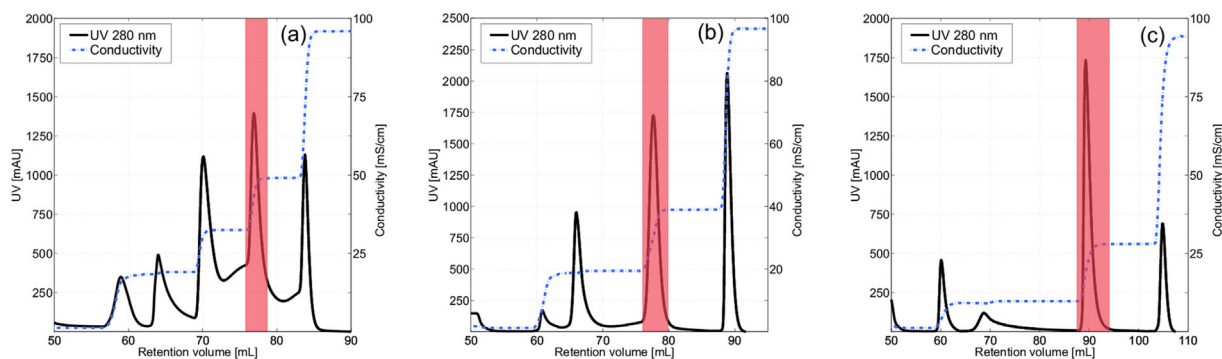


Figure 1. Chromatograms of preparative CEX for 1:12 diluted PEGylation batches ($r = 6.67$, pH 7.2, 3.5 h) loaded with a 50 mL loop for 2 kDa PEG (a), 5 kDa PEG (b), and 10 kDa PEG (c). The red area indicates the respective pooling limits for the mono-PEGylated species.

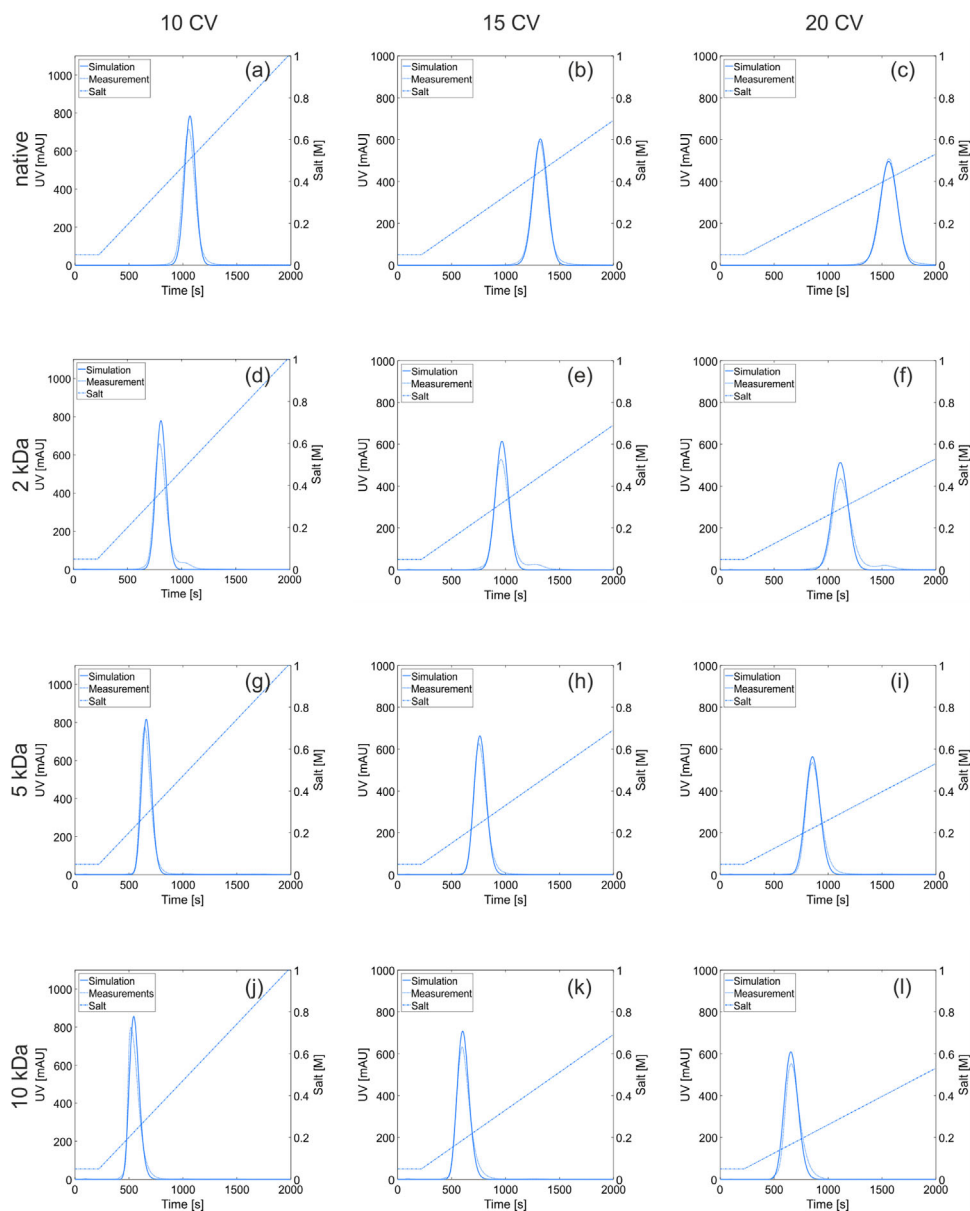


Figure 2. Plots of UV signals over process run-time for bind-and-elute experiments. Dashed lines display the UV signals measured at the column outlet and the adjusted linear salt gradients. Solid lines represent the simulated chromatograms. The elution peaks of native lysozyme, lysozyme attached with 2 kDa PEG, 5 kDa PEG, and 10 kDa PEG by applying linear salt gradients from 0.05 M to 1.0 M over 10 CV, 15 CV, and 20 CV are shown in (a)–(c), (d)–(f), (g)–(i), and (j)–(l). Similar peak heights and widths, but different retention times can be seen for different protein species. Here, the Toyoscreen column was employed.

Comparison of the elution peaks of native and PEGylated species at a constant gradient length in Figure 2 reveals that the elution times decreased with increasing PEG chain length. Except for the different elution times of all protein species, their peak heights and widths are highly similar at each salt gradient conditions. A small shoulder peak behind the main peak can be seen in Figure 2d–f, indicating a small amount of a stronger binding protein species. Presumably this species is by unmodified lysozyme, since for the 2 kDa PEGylation no peak baseline separation between the different PEGamer species

could be achieved in preparative chromatography (compare Figure 1a).

Additionally, breakthrough experiments were carried out under strong binding condition. The 280 nm signals were highly non-linear above 2000 mAU and reached the detector saturation at approximately 2500 mAU. As shown by the dashed lines in **Figure 3**, lysozymes with 10, 5, and 2 kDa PEG attached, and the native lysozyme exhibited their breakthrough in successive order. Based on this information, the shielding parameter σ was estimated and the correlation between k_{kin} and k_{film} that both

Table 2. For the Toyoscreen column, the voidages and axial dispersion are calculated from the retention volume and peak broadening of tracer injections.

GigaCap S-650M		
Particle diameter	d_p	75 μm
Bed voidage	ε_b	0.414
Particle voidage	ε_p	0.779
Total voidage	ε_t	0.871
Axial dispersion [$\text{mm}^2 \text{s}^{-1}$]	D_{ax}	$6.691 \cdot 10^{-2}$
Ionic capacity [M]	Λ	1.389

The ionic capacity is determined by acid–base titration.

affect the peak height in the linear part of the adsorption isotherm was dissolved.

The final parameter estimates and the related confidence intervals at 95% level are summarized in **Table 3**. The simulated LGE for the four protein species are displayed in Figure 2 as solid lines. In all cases, a good agreement between simulations and measurements was found for the retention time, peak width, and peak shape. Overall, the conformity was highest for the native lysozyme. The peak heights of PEGylated species were slightly overestimated. The simulated breakthrough curves for all protein species are displayed in Figure 3. Here, the model accurately accounted for the overall slopes and reflected the process relevant times at 10 and 50% breakthrough. The relative offsets for the process times at 10% breakthrough were 1.83% for lysozyme in the native condition, 3.53% for lysozyme attached with 2 kDa PEG, 1.93% for lysozyme attached with 5 kDa, and 4.17% for lysozyme attached with 10 kDa.

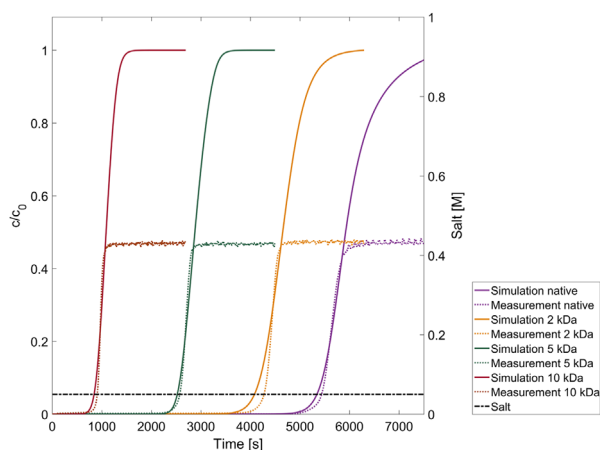


Figure 3. Plots of normalized protein concentration over process runtime for breakthrough experiments. Dashed lines display the normalized protein concentrations calculated from UV signals measured at the column outlet and the constant salt concentration at 0.05 M. Solid lines represent the normalized protein concentrations calculated from the simulated chromatograms. The native lysozyme and lysozyme attached with 2 kDa PEG, 5 kDa PEG, and 10 kDa PEG are shown in purple, yellow, green, and red, respectively. Here, the Toyoscreen column was employed.

3.4. Mass Transfer and Kinetic Phenomena

The GRM assumes that the adsorbent particles have a spherical shape and a uniform diameter. The shape of PEGylated proteins is influenced by the surrounding PEG layer which is highly dynamic. Due to the high hydration of PEG, PEGylated proteins have a significantly greater hydrodynamic radius than unmodified proteins with a comparable molecular weight. Fee and Van Alstine introduced a non-linear relationship between the degree of PEGylation in terms of total molecular weight of PEG attached and the hydrodynamic radius of the PEGylated protein.^[5,8] This non-linearity is the reason why the behavior of conjugated proteins in IEX must necessarily be described as a function of the hydrodynamic radius and not in terms of the total molecular weight of attached polymer. According to the correlation introduced by Fee and Van Alstine,^[5] the hydrodynamic radii $h_{R,PEGprot}$ were calculated to be 2.00, 2.37, 3.08, and 3.84 nm for the four lysozyme species with increasing PEG MW.

For lysozyme, the mass transfer coefficient k_{eff} calculated according to $1/k_{eff} = 1/k_{pore} + 1/k_{film}$ with the internal mass transfer resistance $k_{pore} = 10D_{pore}\varepsilon_p/d_p$ ^[36] was found to be consistent with the literature data.^[35] An approximately linear decrease of the film diffusion coefficient k_{film} with increasing $h_{R,PEGprot}$ was determined as displayed in **Figure 4a**. A comparable dependency was reported by Meja-Manzano et al.^[37] for affinity chromatography. As shown in Figure 4b, the pore diffusion coefficient D_{pore} decreased reciprocally with increasing $h_{R,PEGprot}$ according to the Stokes–Einstein equation qualitatively. The adsorption and desorption rate coefficients $k_{ads} = k_{eq} \setminus k_{kin}$ and $k_{des} = 1 \setminus k_{kin}$ were calculated and are displayed in Figure 4c and d. With increasing PEG MW, both k_{ads} and k_{des} showed an exponential increase. A similar trend has been observed by Meja-Manzano et al.^[37] for affinity chromatography. The increase of k_{des} exceeded the increase of k_{ads} by more than two orders of magnitude. For native and 5 kDa mono-PEGylated lysozyme, k_{eq} was found to be of the same magnitude as reported in the literature.^[11]

3.5. Characteristic Charge and Shielding

The characteristic charges ν of PEGylated lysozyme (4.20–4.22) were found to be equal to the value determined for native lysozyme (4.21) as shown in Figure 4e. ν was unaffected by PEGylation degree and PEG chain length. This finding was consistent with data delivered by Abe and co-worker.^[11] A small shielding factor σ of 5.61 was found for the native lysozyme. With increasing PEG chain length, σ increased from 6.81 for 2 kDa to 9.79 for 5 kDa, and up to 25.90 for 10 kDa PEG as displayed in Figure 4f. The dependency of σ on the hydrodynamic radius was highly non-linear. Based on the definition of q_{max} being $\Lambda(\sigma + \nu)$, the maximal binding capacity q_{max} for the four protein species was calculated to be $1.41 \cdot 10^{-1}$ M for native species, $1.26 \cdot 10^{-1}$ M for 2 kDa PEGylated species, $9.93 \cdot 10^{-2}$ M for 5 kDa PEGylated species and $4.61 \cdot 10^{-2}$ M for 10 kDa PEGylated species. q_{max} was found to be reduced by 10.6% when attached with 2 kDa PEG by 29.6% when attached with 5 kDa PEG, and by 67.3% when attached with 10 kDa PEG compared to the native lysozyme species.

Table 3. Parameters of the mass transfer model and kinetic isotherm formulation estimated from bind-and-elute experiments with linear salt gradient and breakthrough curves using the inverse method are shown for native and mono-PEGylated lysozyme species.

Parameter	Native	2 kDa PEGylated	5 kDa PEGylated	10 kDa PEGylated
k_{film} [mm s ⁻¹]	$9.95 \cdot 10^{-2} \pm 5.20 \cdot 10^{-2}$	$8.92 \cdot 10^{-2} \pm 5.49 \cdot 10^{-2}$	$6.62 \cdot 10^{-2} \pm 3.12 \cdot 10^{-2}$	$4.07 \cdot 10^{-2} \pm 2.53 \cdot 10^{-2}$
D_{pore} [mm ² s ⁻¹]	$2.85 \cdot 10^{-4} \pm 2.38 \cdot 10^{-5}$	$1.33 \cdot 10^{-4} \pm 7.56 \cdot 10^{-6}$	$8.42 \cdot 10^{-5} \pm 2.08 \cdot 10^{-6}$	$5.75 \cdot 10^{-5} \pm 2.28 \cdot 10^{-6}$
k_{eq} [sM ^{<i>v</i>}]	$4.62 \cdot 10^{-2} \pm 9.16 \cdot 10^{-5}$	$5.94 \cdot 10^{-3} \pm 2.79 \cdot 10^{-5}$	$1.16 \cdot 10^{-3} \pm 5.13 \cdot 10^{-6}$	$1.92 \cdot 10^{-5} \pm 1.48 \cdot 10^{-6}$
k_{kin} [-]	$3.94 \cdot 10^{-2} \pm 7.56 \cdot 10^{-4}$	$4.58 \cdot 10^{-3} \pm 2.10 \cdot 10^{-4}$	$2.31 \cdot 10^{-4} \pm 6.74 \cdot 10^{-5}$	$6.34 \cdot 10^{-6} \pm 2.82 \cdot 10^{-5}$
v [-]	$4.21 \pm 1.82 \cdot 10^{-3}$	$4.21 \pm 2.65 \cdot 10^{-3}$	$4.20 \pm 1.10 \cdot 10^{-3}$	$4.22 \pm 1.56 \cdot 10^{-3}$
σ [-]	$5.61 \pm 1.27 \cdot 10^{-2}$	$6.81 \pm 1.35 \cdot 10^{-2}$	$9.79 \pm 1.67 \cdot 10^{-2}$	$25.90 \pm 1.08 \cdot 10^{-1}$

Confidence intervals at 95% level reflect the reliability of the parameter estimates.

4. Discussion

PEGylation is commonly used in biopharmaceutical industry to improve protein stabilities and pharmacokinetics of protein drugs. However, the currently used reaction mechanisms and conditions usually result in a heterogeneous product mixture of unreacted protein and conjugates with varying number and modification site of attached polymers.^[5,6] For this reason, purification processes of PEGylated proteins are imperative. Chromatographic processes based on electrostatic interactions, e.g., ion-exchange chromatography, are among the most effective purification processes for this application.^[12] So far, the development of ion-exchange steps for the purification of the individual PEGamers has been driven mainly by expert-based or experimental approaches (high-throughput process development and statistical design of experiments). These approaches are time-consuming and cost-intensive due to the wide variety of proteins and polymers (linear vs.

branched, molecular weight, etc.). Mechanistic modeling and simulations can help to reduce the number of experiments during process optimization by in silico predictions.^[38] From the perspective of process development, the parameters estimated by mechanistic modeling can be used for process up scaling, process optimization, and process control, meeting the demands of the Quality by Design approach (QbD) proposed by the US food and drug administration (FDA).^[39]

In our work, the SMA isotherm in kinetic formulation coupled with the GRM produced a comprehensive description of the adsorption and desorption behavior on the adsorber surface, steric hindrance, and the mass transfer for native lysozyme and its PEGylated species. The model parameters k_{film} , D_{pore} , k_{eq} , k_{kin} , v , and σ were determined and k_{ads} , k_{des} , $h_{R,PEGprot}$, and q_{max} were calculated to improve the mechanistic understanding of PEGylated proteins in CEX. It should be mentioned, that the PEGylation reaction usually delivers various PEGamer isoforms. In the

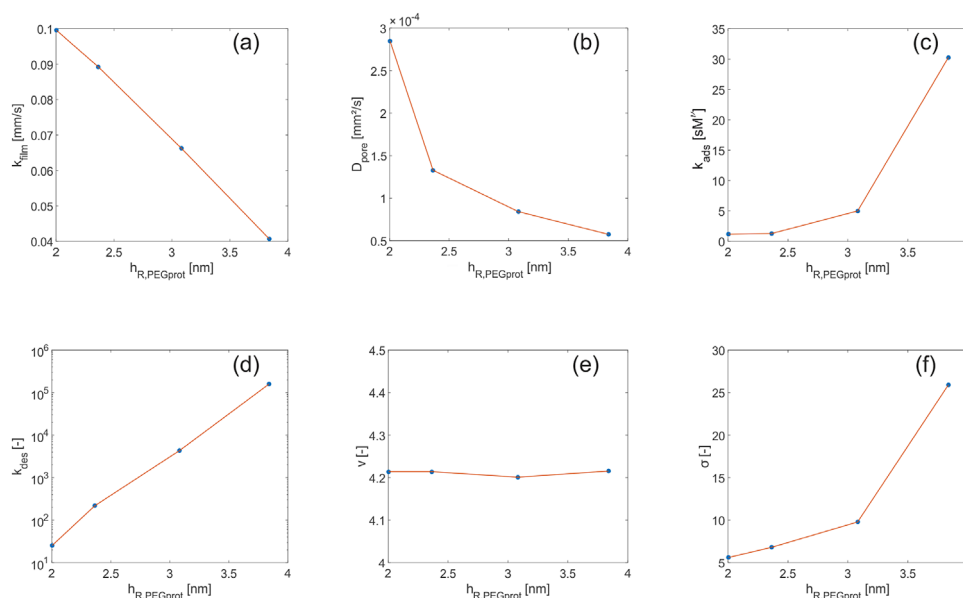


Figure 4. a–f) The show film diffusion coefficient, pore diffusion coefficient, adsorption coefficient, desorption coefficient, characteristic charge, and shielding factor versus the hydrodynamic radius $h_{R,PEGprot}$ of PEGamers. $h_{R,PEGprot}$ takes into account the non-linear relationship between conjugate size and total molecular weight of attached PEG.^[5,8] Blue dots from left to right represent the native lysozyme and lysozyme attached with 2 kDa PEG, 5 kDa PEG, and 10 kDa PEG.

presented case, the isoforms behaved highly similar and could not be separated with the used CEX setup. Hence all isoforms of each lysozyme species had to be modeled as lumped components, resulting in slight overestimation of the peak heights.

As reported by many researchers, PEGylated proteins elute earlier than their native analogs.^[9,11,12] Based on the observation of the elution order of different PEGylated species being the same in both cation- and anion-exchange chromatography, Seely and Richey suggested the “charge-shielding effect” to explain this phenomenon.^[9] Later, Abe and co-workers applied the equilibrium stoichiometric displacement isotherm model (SDM) to describe the retention time of PEGylated proteins in linear gradient experiments and determined similar numbers of binding sites for lysozyme and BSA attached with PEG of different lengths. Furthermore, they reported the decrease of a lumped parameter consisting of the equilibrium coefficient, the binding site, and the ionic binding capacity with increasing PEG chain length.^[11] In this way, the “charge-shielding effect” hypothesis was verified and the equilibrium coefficient was identified to be responsible for the weaker binding of PEGylated proteins.^[11]

k_{film} showed a linear dependency on $h_{R,PEGprot}$ as expected according to the correlation suggested by Jungbauer and Carta.^[25] Its decrease with increasing PEG chain length was to be reflected by broader and lower elution peaks. However, the LGE under same operating conditions showed similar peak heights and widths for all PEGylated and native species. Considering the fact that there is a strongly exponential correlation of k_{des} with $h_{R,PEGprot}$, a diffusion-desorption-compensation effect is suggested to be responsible for the uniformity in peak heights and width. The faster desorption of proteins attached with longer PEG chain may be neutralized by the slower film diffusion. This hypothesis is highly consistent with the widely accepted view of the “charge-shielding effect”, since weaker charged proteins increasingly tend to undergo desorption. D_{pore} showed a reciprocal correlation with $h_{R,PEGprot}$, as had been expected according to the Stokes–Einstein equation,^[40] which is reflected by slight tailing of elution peaks in LGE. D_{pore} was found to exceed the molecular diffusion coefficient for native lysozyme. As intensively studies in the literature, there are two opinions to explain this effect. Carta et al. and Rodrigues et al.^[41–43] introduced the convection-enhanced effective intra-particle diffusivity. Many more experimental examples of intra-particle convection in protein chromatography could be found in the literature.^[44–48] However, convective mass transfer into the bead interior was observed for large pores (>5000 Å).^[48,49] For small pores up to 700 Å, Nash et al. assumed diffusional mass transport only. For the TOYOPEARL® GigaCap S-650M resin having an average pore size of 1000 Å, the observed molecular diffusion coefficient cannot be explained completely by convective mass transport in the pores. An additional effect observed by Dziennik et al.^[50] for porous resins with high charge density applies to TOYOPEARL® GigaCap S-650M. They found indications that non-diffusive mechanisms of electrostatic origin could enhance protein uptake rates in ion exchange particles, resulting in enhanced effective pore diffusivities.

The shielding factor σ showed an exponential increase with increasing PEG chain length. In comparison to native lysozyme, approximately 12, 43, and 207% more free binding sites are sterically hindered by the species with 2, 5, and 10 kDa PEG

attached, respectively. In contrast to this, ν was found to be independent of PEGylation and PEG chain length, indicating the same binding orientation for all species. Thus, the steric hindrance of free binding sites was identified to be the main contributor to the observed exponential decrease of molar binding capacity q_{max} upon PEGylation. It is indicated that the longer PEG chains of an adsorbed protein make many more free binding sites inaccessible than the shorter ones or equally sized unmodified proteins. Fee and Van Alstine proposed a correlation for the average shape of the PEG-layers around a protein over time scale.^[5,6] These layers are expected to have increasing degree of dynamics with increasing PEG molecular weight.^[51] This concept could also explain the non-linearity in k_{ads} , k_{des} , and σ shown in Figure 4c, d, and f.

Especially in the overloading state under strong binding condition, a high density of proteins bound could result in formation of multiple PEG chain layers covering adjacent free binding sites. The multiple PEG chain layers would not shield the electrostatic interactions, but keep the proteins in the mobile phase distant from the adsorber surface, so that the electrostatic attraction would become weak and binding impossible. This hypothesis is schematically represented by Figure 5. Along the increasing binding density, several transitional states are supposed to exist. First, in the linear

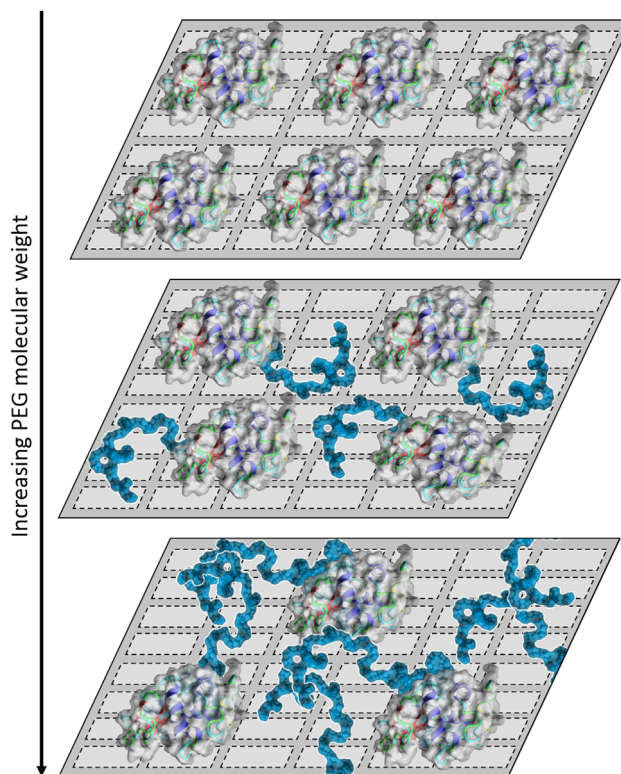


Figure 5. Molecular picture of the adsorption of lysozymes on an adsorber surface. Increasing PEG chain length results in the formation of multiple PEG chain layers hindering the binding of further lysozymes. The reduction of accessible binding sites explains the observed decrease in binding capacity upon protein PEGylation. (Molecular graphic of lysozyme (PDB: 1LYZ) was created with YASARA (www.yasara.org)).

part of the adsorption isotherm, the proteins could distribute uniformly on the adsorber surface; secondly, unfavorable binding sites between the proteins covered by thin PEG chain layers could be occupied, though the electrostatic attraction could already be reduced; finally, the multiple PEG chain layers could become dominant, so that the electrostatic attraction could disappear and binding could be suppressed. This concept is consistent with the observation made by Blaschke and co-workers.^[52] They found that adsorption was less enthalpy-driven at higher loading states for proteins attached with longer PEG chains.

Of course, the PEG-layers around PEGylated proteins are not static, rather of dynamic nature. Thus, the mechanistic chromatography model describes the average behavior of lysozyme species in CEX. As suggested by Fee et al., the dynamicism of PEG-layers tend to increase with increasing PEG chain length. This concept could be an alternative explanation for the nontrivial behavior of PEGylated lysozymes observed in the presented work.

Using mechanistic chromatography modeling and considering insights provided by former pioneer work, the hydrodynamics and thermodynamics of PEGylated lysozymes in CEX were investigated. The diffusion-desorption-compensation effect was introduced to explain the anomaly of peak heights and widths remaining constant in spite of an increasing hydrodynamic radius. Additionally, it reflects the exponential dependency of the shielding factor on the MW of PEGylated proteins and suggests that multiple PEG chain layers formed in the overloading state are responsible for this non-trivial phenomenon. Thus, the model view of PEGylated proteins' behavior in CEX was supplemented by the overloading state.

This study clearly demonstrates that mechanistic chromatography modeling can be applied to describe PEGylated proteins with high accuracy and reliability. Thus it has great potential for the optimization, prediction and scale-up of purification processes for PEGylated proteins. A future challenge is to show whether the separation of positional isoforms can be predicted by this kind of simulation. In this respect, a combination of mechanistic chromatography modeling combined with molecular modeling could be profitable.

Supporting Information

Supporting Information is available from the Wiley Online Library or from the author.

Acknowledgements

J.M. and G.W. contributed equally to this work. This project partly received funding from the European Union's Horizon 2020 Research and Innovation Programme under grant agreement no. 635557. Furthermore, we would like to acknowledge the further financial support by the German Federal Ministry of Education and Research (BMBF) within the project "Molecular Interaction Engineering: From Nature's Toolbox to Hybrid Technical Systems", funding code 031A095B. We want to thank Carina Brunner for her reliable and persistent support in the laboratory. Last but not least, we kindly thank Johannes Winderl for useful discussions related to this work.

Conflict of Interest

The authors declare no commercial or financial conflict of interest.

Keywords

diffusion-desorption-compensation effect, ion-exchange chromatography, mechanistic modeling, PEGylated proteins, shielding

Received: March 28, 2017

Revised: July 5, 2017

Published online: August 14, 2017

- [1] EvaluatePharma, World preview2015, outlook to 2020 (Dec. 2016). URL <http://info.evaluategroup.com/rs/607-YGS-364/images/wp15.pdf>.
- [2] J. M. Harris, R. B. Chess, *Nat. Rev. Drug Discov.* **2003**, 2, 214.
- [3] A. Abuchowski, T. Van Es, N. Palczuk, F. Davis, *J. Biol. Chem.* **1977**, 252, 3578.
- [4] J. Morgenstern, P. Baumann, C. Brunner, J. Hubbuch, *Int. J. Pharm.* **2017**, 519, 408.
- [5] C. J. Fee, J. M. V. Alstine, *Chem. Eng. Sci.* **2006**, 61, 934.
- [6] J.-C. Janson, "Protein Purification: Principles, High Resolution Methods, and Applications", Vol. 151, John Wiley & Sons, Hoboken, New Jersey, **2012**, Ch. 14.
- [7] G. Pasut, F. M. Veronese, *J. Control. Release* **2012**, 161, 461.
- [8] C. J. Fee, J. M. Van Alstine, *Bioconj. Chem.* **2004**, 15, 1304.
- [9] J. E. Seely, C. W. Richey, *J. Chromatogr. A* **2001**, 908, 235.
- [10] S. Yamamoto, S. Fujii, N. Yoshimoto, P. Akbarzadehlaleh, *J. Biotechnol.* **2007**, 132, 196.
- [11] M. Abe, P. Akbarzadehlaleh, M. Hamachi, N. Yoshimoto, S. Yamamoto, *Biotechnol.* **2010**, 5, 477.
- [12] N. Yoshimoto, Y. Isakari, D. Itoh, S. Yamamoto, *Biotechnol. J.* **2013**, 8, 801.
- [13] C. A. Brooks, S. M. Cramer, *AIChE J.* **1992**, 38, 1969.
- [14] G. Guiochon, L. A. Beaver, *J. Chromatogr. A* **2011**, 1218, 8836.
- [15] T. Hahn, T. Huuk, V. Heuveline, J. Hubbuch, *J. Chem. Educ.* **2015**, 92, 1497.
- [16] J. Morgenstern, M. Busch, P. Baumann, J. Hubbuch, *J. Chromatogr. A* **2016**, 1462, 153.
- [17] B. Maiser, F. Dismer, J. Hubbuch, *Biotechnol. Bioeng* **2014**, 111, 104.
- [18] K. E. Ottow, T. Lund-Olesen, T. L. Maury, M. F. Hansen, T. J. Hobbey, *Biotechnol. J.* **2011**, 6, 396.
- [19] PerkinElmer, Labchip gx/gx ii—user manual (Jan. 2017). URL http://www.perkinelmer.com/Content/LST_Software_Downloads/LabChip_GX_User_Manual.pdf.
- [20] K. Baumgartner, L. Galm, J. Nötzold, H. Sigloch, J. Morgenstern, K. Schleining, S. Suhm, S. A. Oelmeier, J. Hubbuch, *Int. J. Pharm.* **2015**, 479, 28.
- [21] H. Research, Lysozyme—user guide hr7-110 (Jan. 2017). URL http://hamptonresearch.com/documents/product/hr006812_711020.pdf.
- [22] T. C. Huuk, T. Briskot, T. Hahn, J. Hubbuch, *Biotechnol. Progr.* **2016**, 32, 666.
- [23] A. Velayudhan, *J. Chromatogr. A* **1988**, 443, 13.
- [24] N. Jakobsson, D. Karlsson, J. P. Axelsson, G. Zacchi, B. Nilsson, *J. Chromatogr. A* **2005**, 1063, 99.
- [25] G. Carta, A. Jungbauer, *Protein Chromatography Process Development and Scale-Up*, WILEY-VCH, Weinheim, **2010**.
- [26] A. M. Lenhoff, *J. Chromatogr. A* **2011**, 1218, 8748.
- [27] A. Wittemann, B. Haupt, M. Ballauff, *Phys. Chem. Chem. Phys.* **2003**, 5, 1671.

- [28] T. Hahn, P. Baumann, T. Huuk, V. Heuveline, J. Hubbuch, *Eng. Life Sci.* **2016**, 16, 99.
- [29] K. Kaczmariski, D. Antos, *Acta Chromatogr.* **2006**, 17, 20.
- [30] F. Devernay, C/C++ minpack, <http://devernay.free.fr/hacks/cminpack/> **2007**.
- [31] R. Glowinski, *Flow in Numerical Methods for Fluids (Part 3)*, Volume IX, Elsevier, North-Holland, **2003**.
- [32] A. Quarteroni, A. Valli, *Numerical Approximation of Partial Differential Equations*, Springer, Heidelberg, **1994**.
- [33] B. Maiser, F. Kröner, F. Dismar, G. Brenner-Weiß, J. Hubbuch, *J. Chromatogr. A* **2012**, 1268, 102.
- [34] N. Yoshimoto, S. Yamamoto, *Biotechnol. J.* **2012**, 7, 592.
- [35] G. Wang, T. Briskot, T. Hahn, P. Baumann, J. Hubbuch, *J. Chromatogr. A* **2017**, 1487 501, 211.
- [36] H. Schmidt-Traub, M. Schulte, A. Seidel-Morgenstern, *Preparative Chromatography*, 2nd Edition, WILEY-VCH, Weinheim, **2012**.
- [37] L. A. Mejía-Manzano, G. Sandoval, M. E. Lienqueo, P. Moisset, M. Rito-Palomares, J. A. Asenjo, *J. Chem. Technol. Biotechnol.* **2017**. <https://doi.org/10.1002/jctb.5309>
- [38] B. K. Nfor, P. D. Verhaert, L. A. M. van der Wielen, J. Hubbuch, M. Ottens, *Trend Biotechnol.* **2009**, 27, 673.
- [39] International Conference on Harmonisation of Technical Requirements for Registration of Pharmaceuticals for Human Use, ICH-Endorsed Guide for ICH Q8/Q9/Q10 Implementation, http://www.ich.org/fileadmin/Public_Web_Site/ICH_Products/Guidelines/Quality/Q8_9_10_QAs/PtC/Quality_IWG_PtCR2_6dec2011.pdf.
- [40] A. Einstein, *Ann Phys.* **1905**, 17, 549.
- [41] G. Carta, M. E. Gregory, D. J. Kirwan, *Sep. Technol.* **1992**, 2, 62.
- [42] G. Carta, A. E. Rodrigues, *Chem. Eng. Sci.* **1993**, 48, 3927.
- [43] A. E. Rodrigues, Z. P. Lu, J. M. Loureiro, G. Carta, *J. Chromatogr. A* **1993**, 653, 189.
- [44] D. D. Frey, E. Schweinheim, C. Horvath, *Biotechnol. Progr.* **1993**, 9, 273.
- [45] R. Freitag, D. Frey, C. Horvath, *J. Chromatogr. A* **1994**, 686, 165.
- [46] J. F. Pfeiffer, J. C. Chen, J. T. Hsu, *AIChE J.* **1996**, 42, 932.
- [47] P. E. Gustavsson, K. Mosbach, K. Nilsson, P. O. Larsson, *J. Chromatogr. A* **1997**, 776, 197.
- [48] D. C. Nash, H. A. Chase, *J. Chromatogr. A* **1998**, 807, 185.
- [49] L. L. Lloyd, *J. Chromatogr. A* **1991**, 544, 201.
- [50] S. R. Dziennik, E. B. Belcher, G. A. Barker, M. J. DeBergalis, S. E. Fernandez, A. M. Lenhoff, *PNAS* **2003**, 100, 420.
- [51] J. M. Van Alstine, M. Malmsten, *Langmuir* **1997**, 13, 4044.
- [52] T. Blaschke, J. Varon, A. Werner, H. Hasse, *J. Chromatogr. A* **2011**, 1218, 4720.